Contrasting responses of soil inorganic carbon to afforestation in acidic versus alkaline soils

Songbai Hong[a] & Anping Chen[b*]

[a] Sino-French Institute for Earth System Science, College of Urban and Environmental Sciences, Peking University, Beijing 100871, China (email: songbaih@pku.edu.cn)

[b] Department of Biology and Graduate Degree Program in Ecology, Colorado State University, Fort Collins, CO 80523, USA (email: anping.chen@colostate.edu)

[*] Correspondence author, Email: anping.chen@colostate.edu
Tel: (+1) 970-495-5272
Fax: (+1) 970-491-0649

Article type: Research Article

Key Points:

- We conducted an extensive field survey investigating the impact of afforestation on soil inorganic carbon (SIC)
- Soil pH is a key variable mediating SIC responses to afforestation, which enhanced SIC in acidic soils but decreased SIC in alkaline soils
- SIC responses to afforestation also showed high variabilities among different planted tree species and across soil depths

Abstract

Afforestation has been suggested as an effective ecological engineering approach for carbon sequestration and environmental benefits. However, the impact of afforestation on soil inorganic carbon (SIC) is less clear and sometimes controversial. Here, we conducted a field campaign, with 2346 soil profiles from 619 afforested plots and 163 control plots, to investigate the relative and absolute changes of SIC between afforested and corresponding control plots in northern China. We found positive responses of SIC to afforestation in acidic soils, where afforestation increased soil pH. In contrast, in alkaline soil, afforestation caused soil acidification and thus negative SIC responses. Fitting a structure equation model (SEM) confirmed that afforestation-induced soil pH change (ΔpH) was the most significant factor regulated SIC responses to afforestation. In particular, we observed stronger SIC sensitivity to pH change in arid areas, where both soil pH and SIC stocks were high. Other factors indirectly affected SIC responses to afforestation through modulating soil pH and soil organic carbon (SOC) dynamics. Afforestation-induced SIC changes also varied considerably among different planted tree species and across different soil depths. Specifically, in *Pinus sylvestris* var. *mongholica*, *Pinus tabuliformis* and *Populus* spp. plantations, changes of SIC were large enough to be comparable to that of SOC. Our finding provides a data-based comprehensive understanding on the impact of afforestation on SIC and its underlying mechanisms. With increased uses of afforestation and reforestation as potential nature-based climate solutions, decisions need to consider potential associated SIC changes, especially in SIC-rich areas.

Key words: Plant–soil interactions; afforestation; soil inorganic carbon (SIC); soil pH; structural equation model; nature-based climate solution

1. Introduction

About 950 petagrams (Pg) carbon is stored in global soils in inorganic formula (Schlesinger & Andrews, 2000; Lal, 2004), even more than that of vegetation carbon (Schlesinger, 1990; Ahirwal & Maiti, 2018). This large soil inorganic carbon (SIC) pool is usually considered stable and thus plays a very limited role in global carbon cycle (Zamanian et al., 2018). However, several recent local-scale studies showed considerable SIC responses to agricultural management and land use changes, thus challenging this conventional notion (Bughio et al., 2016; Han et al., 2018; An et al., 2019; Kim et al., 2020). For example, SIC is found sensitive to soil acidification, which is often caused by nitrogen deposition and fertilization, and to land use changes and shrub encroachment (Yang et al., 2012b; Liu et al., 2020). Because SIC provides important soil buffering especially in alkaline soils (Bowman et al., 2008), its changes could modify soil buffering capacity and soil pH (Bowman et al., 2008; Yang et al., 2012b; Hong et al., 2019), and thus impact soil health and consequently vegetation productivities (Skyllberg, 1996; Yang et al., 2012a; Chang et al., 2012; Bughio et al., 2016; Bughio et al., 2017; Liu et al., 2020). Yet, to date, research on SIC dynamics is still very limited, especially for large-scale investigations of SIC responses to decadal land use changes that have been a key feature characterizing global environmental changes (IPCC AR5, 2014; Piao et al., 2018).

Afforestation has been extensively adopted in many countries and regions during the past decades for economic, ecological and climate change mitigation purposes (Bonan, 2008). Afforestation can reduce soil erosion (Fang & Sun, 2017), regulate

local and regional climate (Peng et al., 2014; Li et al., 2018; Li et al., 2020) and enhance carbon sequestration (Fang et al., 2001; Chang et al., 2011). The increase of vegetation biomass by afforestation has been reported by many studies (e.g., Fang & Chen, 2001; Piao et al., 2005; Pan et al., 2011). Afforestation is also suggested to increase soil organic carbon (SOC; Cheng et al., 2016; but see Hong et al., 2020). However, it remains poorly understood how afforestation may influence SIC (Jia et al., 2019). In principle, afforestation may affect SIC through several different mechanisms and processes (Figure 1). First, afforestation could modify soil pH (Rhoades & Binkley, 1996; Berthrong et al., 2009; Hong et al., 2018), a key variable that is significantly correlated with SIC stocks (Bowman et al., 2008; Hong et al., 2019). For instance, afforestation-induced soil acidification is generally observed on soils with relatively higher pH, where SIC stock is usually high (Yang et al., 2012a; Hong et al., 2018; Hong et al., 2019). In return, this soil acidification can lead to the loss of SIC. Second, for locations where afforestation enhances SOC, the increase of SOC could stimulate soil microbial respiration and release more porous CO_2 gases and Ca^{2+} and Mg^{2+} ions, all of which may modulate the dissolution and re-precipitation of carbonates (An et al., 2019). Third, afforestation changes land surface roughness and hence affects ecosystem intercept of nitrogen deposition (HÖGberg et al., 2006). With more intercepted nitrogen deposition, the leaching of base cations may increase as well, which could also impact the dynamics of SIC (Gundersen et al., 2011). Fourth, afforestation increases evapotranspiration and decreases the infiltration of soil water (Yao et al., 2016), which may reduce SIC losses through leaching. While all these

processes have the potential to regulate the responses of SIC to afforestation toward different directions, however, we know little about the overall afforestation impact on SIC, and how to quantitatively attribute SIC changes to different processes.

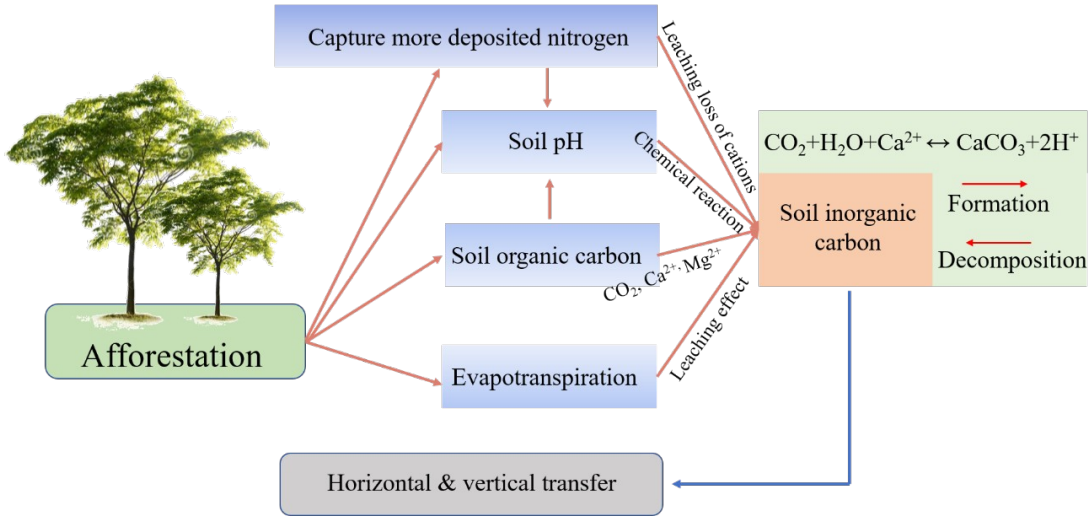

Figure 1. A concept diagram on how afforestation affects soil inorganic carbon.

In this study, we used a control-afforestation paired sampling in northern China to investigate how afforestation impacts SIC. In 2012-2013, we collected soils from 163 control plots and 619 afforested plots across northern China (see Figure 2 for field sampling locations), with each control plot corresponding to 1-26 afforested plots. These plots thus were used to construct 619 afforestation-control pairs for comparative investigations of SIC changes with versus without afforestation. Using a structure equation model (SEM) that links the SIC responses to afforestation with various environmental factors, we also researched potential mechanisms how afforestation affects SIC dynamics. We further explored the contribution of SIC changes to soil carbon dynamics under afforestation. Our results provide a

112 comprehensive understanding of SIC dynamics with afforestation, and highlights the
113 significant role of SIC in ecosystem carbon cycle.
114
115 **2. Materials and methods**
116 **2.1 Study region**
117 Field work was conducted in northern China (34.20 to 51.80°N and 106.81 to
118 133.31°E; Figure 2), where afforestation and ecological restoration projects have been
119 widely implemented. The region covers the provinces of Heilongjiang, Jilin,
120 Liaoning, Hebei, Shanxi, and Shaanxi Provinces and the Inner Mongolia Autonomous
121 Region. It contains more than 120,000 km^2 of forest plantations, including the well-
122 known Three-North Shelterbelt Development Program (Piao et al., 2009; FAO, 2016).
123 Climate in this large area is highly various, with mean annual temperature (MAT)
124 ranging from −3 to 15 °C and mean annual precipitation (MAP) from 355 to 1068
125 mm. Dominant soil types in this region include phaeozems, gleysols, humic
126 cambisols, haplic/albic luvisols or eutric/dystric cambisols, haplic calcisols,
127 kastanozems, chernozems, cambisols, haplic alisols, and ferric/haplic luvisols,
128 following the United Nations Food and Agriculture Organization (FAO) soil
129 classification system (Xiong & Li, 1987; Xie et al., 2007). Intense nitrogen deposition
130 over the last few decades has been reported in this region, with significant impacts on
131 soil properties and plant productivities (Zhao et al., 2009). Overall, these broad-scale
132 afforestation projects, together with northern China's diverse climate and soil
133 properties and intense nitrogen deposition, make this region an ideal place to

investigate afforestation impacts on SIC dynamics across broad geographical and environmental ranges.

2.2 Sampling design

We established a control-afforested pairwise sampling system from 163 sites across the study area. In each site, one control plot and 1-26 afforested plots, each measured at 20 m × 20 m, with different planted tree species or stand ages, were selected. Therefore, one control plot can correspond to more than one afforested plot. To minimize the variation in soil and climatic properties within each control-afforested pair, the distance between any afforested plot and its corresponding control plot was usually 50–100 m (up to 2.5 km in very rare cases due to field or logistic constraints). Following the records provided by local forestry administrations, we also made sure that the selected control plots had the same vegetation and soil types with their corresponding afforested plots. In other words, each paired control and afforested plots shared the same topography, climate, soil type and pre-afforestation vegetation type. The only difference between them was afforestation versus no-afforestation. In total, we obtained data from 163 control plots and 619 afforested plots, which constituted 619 control-afforested pairs. The original vegetation types included cropland, barren land, grassland, natural forest and riparian sand land in this study. All the afforested plots were monocultured, with common tree species including *Pinus koraiensis*, *Larix gmelinii*, *Pinus sylvestris* var. *mongholica*, *Pinus tabuliformis*, and *Populus* species (including *Pop. simonii*, *Pop. beijingensis*, and

156 *Populus* × *xiaohei*), and some other species such as *Robinia pseudoacacia* L. and
157 *Diospyros kaki* Thunb. (collectively grouped as "others"). The five major tree species
158 collectively account for >70% of the planted area in the study region. Information of
159 each plot's stand age was obtained from records of local forestry administrations.
160 For each plot, we sampled from three replicate soil profiles on the diagonal
161 direction, each at six different depths (0-5, 5-10, 10-20, 20-30, 30-60, and 60-100 cm;
162 with a few exceptions when soil depths were less than 1 m). Hence, for any plot we
163 could reach 1-m depth, we had 18 samples (3 replicates × 6 layers per replicate); and
164 in total, we collected 11,775 soil samples from 2,346 soil profiles.
165
166 **2.3 Laboratory method**
167 All soil samples were brought back to the laboratory and air-dried to constant
168 weight, and roots and stones were removed. After that, we measured bulk density and
169 had the samples passed through 2-mm sieves. The pH of each sample was measured
170 in 1:2.5 mixtures of soil and deionized water with a pH meter (PHS-3C, Lei-ci). Soil
171 inorganic C content (SICC) was measured with a 08.53 calcimeter (M1.08.53.E,
172 Eijkelkamp). Here SICC was equivalent to the carbonate values measured by the
173 emission of carbon dioxide (CO_2) when the samples were digested with acid (HCl, 0.2
174 mol L^{-1}). Note for comparison, we also calculated soil organic carbon content
175 (SOCC), which was the difference between total soil C content (STCC; measured
176 with an Elementar model (Viro el cube)) and SICC.
177

2.4 Environmental data sets

The following environmental data sets were used to explore the environmental control of SIC responses to afforestation. MAP and MAT were obtained from the China Meteorological Forcing Dataset, which has a spatial resolution of 0.1 × 0.1° and a temporal resolution of three hours (Yang et al., 2010; Chen et al., 2011). Potential evapotranspiration (PET) data were acquired from the Climate Research Unit (CRU) TS3.21 database with a 0.5°x0.5° spatial resolution (Harris et al., 2014). We further estimated water balance (WB) as the difference between mean annual precipitation and potential evapotranspiration (WB=MAP-PET). It is noteworthy that we used PET rather than actual evapotranspiration (AET) because PET is independent of precipitation and therefore could carry more information of climatic aridity (Slessarev et al., 2016; Lian et al., 2021). We also obtained data of nitrogen deposition from the Multi-Scale Synthesis and Terrestrial Model Intercomparison Project (MsTMIP; https://doi.org/10.3334/ORNLDAAC/1220). This dataset includes ammonium nitrogen (NHx) deposition and nitrate nitrogen (NOx) deposition at a resolution of 0.5° × 0.5° from 1860-2050 and we used data of 2003-2012 (Wei et al., 2014).

2.5 Data analysis

We calculated SIC in layer j (SIC_j, kgC m^{-2}) using $SICC_j$ (%), bulk density (BD_j, g cm^{-3}), and the thickness of the layer (w_j, cm):

$$SIC_j = SICC_j * BD_j * w_j * 10^{-1} \quad (1)$$

200 Since each plot included three replicate profiles, we used mean SIC_j of the three
201 profiles in data analysis. The sum of mean SIC_j for all the layers is thus SIC of each
202 plot:

203 $$SIC = \sum_{j=1}^{6} SIC_j \quad (2)$$

204 We defined ΔSIC induced by afforestation as the difference between SIC in the
205 afforested plots (SIC_f) and that in the control plots (SIC_c) at both the plot and layer
206 levels (Eq. 3). Note that SIC values were corrected to equivalent soil mass since
207 afforestation could also change soil bulk density.

208 $$\Delta SIC = SIC_f - SIC_c \quad (3)$$

209 We defined the response ratio (RR) of SIC as:

210 $$RR_{SIC} = \log_{10}\left(\frac{SIC_f}{SIC_c}\right) \quad (4)$$

211 Here, ΔSIC is the absolute change of SIC while RR_SIC is the relative change.
212 Data of SOC was also calculated in same way and we also defined ΔSOC and
213 RR_SOC:

214 $$\Delta SOC = SOC_f - SOC_c \quad (5)$$

215 $$RR_{SOC} = \log_{10}\left(\frac{SOC_f}{SOC_c}\right) \quad (6)$$

216 Because pH value represents the concentration of hydrogen irons, so the
217 following calculations about soil pH were based on concentration of hydrogen irons.
218 The mean concentration of hydrogen ions (H_p) for the entire soil profile was
219 calculated from hydrogen ion concentration, $[H^+]$, of each layer weighted by its mass

220 (w_j * BD_j):

221 $$H_p = \frac{\sum_{j=1}^{6} H_j * w_j * BD_j}{\sum_{j=1}^{6} w_j * BD_j} \quad (7)$$

222 where H_j is the concentration of hydrogen ions of the jth layer. Similarly, the mean
223 concentration of hydrogen ions in a plot was calculated by averaging H_p of its three
224 replicate profiles, and then we got the average pH for each plot from a log
225 transformation of the average H_p.

226 Changes of soil pH (ΔpH) was calculated by Eq. 8 (pH_f and pH_c indicated
227 the averaged soil pH in afforested and control plots, respectively):

228 $$\Delta pH = pH_f - pH_c \quad (8)$$

229 We first conducted the following statistical analyses to explore the effects of
230 afforestation on SIC. A paired *t*-test was used to compare SIC in the afforested plots
231 with their corresponding control plots. Independent *t*-tests were used to determine if
232 ΔSIC and RR_SIC differed significantly from 0. A false discovery rate (FDR)
233 correction was used to control for potential error rates in multiple comparisons
234 (Benjamini & Yekutieli, 2001). Ordinary least squared (OLS) regressions and partial
235 regressions were performed to identify the relationships between variables.
236 Furthermore, we used a two-way analysis of variance (ANOVA) to test the effect of
237 different factors on the dynamics of SIC.

238 Finally, we fitted piecewise structure equation model (SEM) to explore potential
239 pathways (and mechanisms) through which afforestation may affect SIC. Predictor

variables in the SEM included ΔpH, ΔSOC, pH in control group (pH_c), SOC in control group (SOC_c), SIC in control group (SIC_c), MAT, water balance, NOx, NHx, stand age, and clay content. The overall fit of the SEM was evaluated using Shipley's test of d-separation: Fisher'C statistic and the Akaike Information Criterion (AIC). We used the R package 'piecewiseSEM' in R studio to conduct piecewise SEM. All the other statistical analysis was conducted using MATLAB R2012b (MathWorks, Natick, MA, USA).

3. Results

3.1 Changes of SIC with afforestation

Over the entire study area, the average SIC density (0-1 m depth) was 1.70 kgC m^{-2}, with a very large variation (Figure 2a, SD = 4.20). For most of the data collection (77%), SIC density was found in the range of 0.01-1 kgC m^{-2} (Figure 2a inset). Across the entire region, SIC is about 17% of SOC. However, the SIC: SOC ratio is highly variable and skewed across the region, with most (75%) of the ratio falling in the range of 0-0.1(Figure 2b inset) but an unusually high mean value of 1.23 (Figure 2b, SD = 12.26) due to some locations with extremely higher SIC than SOC. SIC density was higher in relatively arid areas, such as the Inner Mongolia Autonomous Region, Hebei, Shanxi and Shaanxi Provinces.

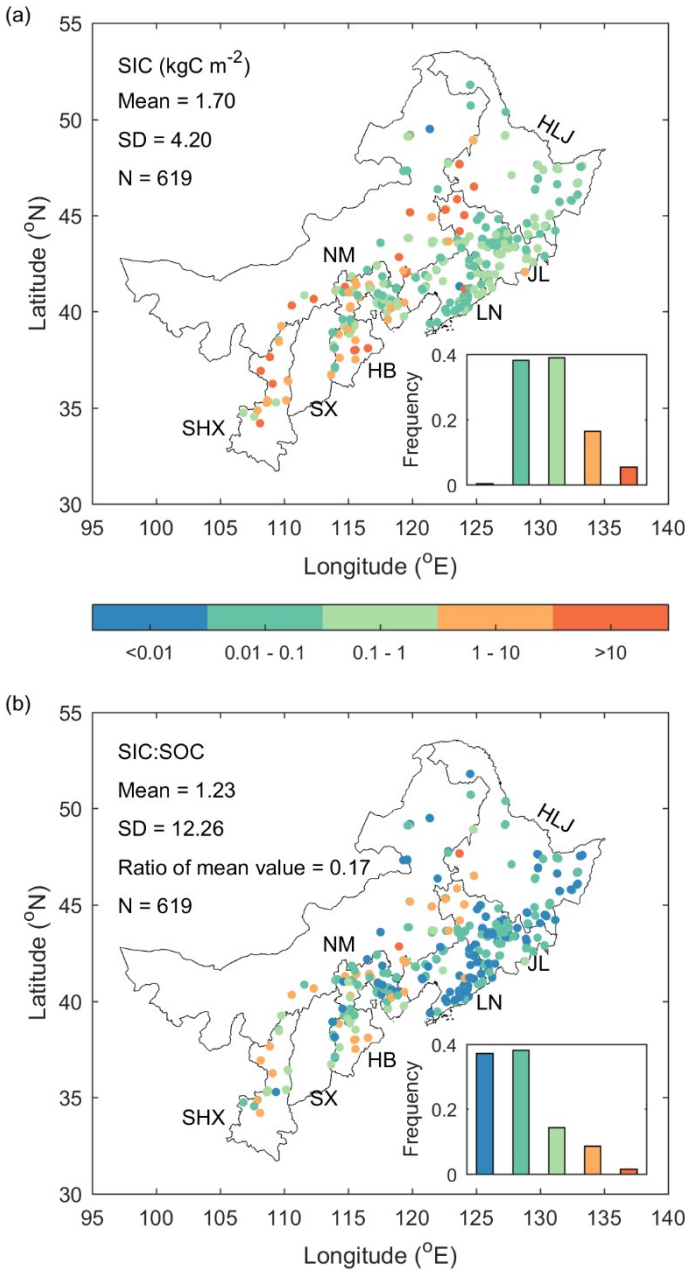

259

260 **Figure 2.** The spatial distributions of (a) soil inorganic carbon (SIC) and (b) the ratios
261 between SIC and soil organic carbon (SOC) in planted forests. The insets show the
262 frequency distributions of the data. Panel (a), (b) and the two insets share the same
263 color bar. Ratio of the mean value indicates the ratio between averaged SIC and
264 averaged SOC across all the plots. NM indicates the Inner Mongolia Autonomous
265 Region, while HL, JL, LN, HB, SX, and SHX indicate the province of Heilongjiang,

Jilin, Liaoning, Hebei, Shanxi, and Shaanxi, Respectively.

Across the 619 afforestation-control pairs, the average of RR_SIC was -0.03 (Figure3, SD = 0.74, p = 0.34), indicating an overall nonsignificant change on SIC with afforestation. Specifically, afforestation decreased SIC in 329 pairs, with the mean SIC of these pairs decreasing from 2.07 to 0.83 kgC m^{-2}. By contrast, SIC was higher in afforested than control plots in the remaining 290 pairs, where the average SIC increased from 1.19 to 2.69 kgC m^{-2}. The overall change of SIC in 0-1 m depth was 0.05 kgC m^{-2} (SD = 3.23, 1.655 in control groups vs. 1.703 in afforested groups, p = 0.71).

The response of SIC to afforestation varied across tree species and depths (Figure 3). In general, afforestation significantly decreased SIC at depths of 0-5 cm, 10-20 cm and 60-100 cm. For other depths, we observed negative but non-significant SIC changes with afforestation. Afforestation with *Pinus koraiensis* resulted in divergent changes of SIC at different depths, although all of them were non-significant. Significantly negative responses of SIC were observed at top soils (0-5 cm) for *Larix gmelinii* and *Pinus tabuliformis* stands. Similarly, afforestation with *Pinus sylvestris* var. *mongholica* caused significant decrease at 0-5 cm and 10-20 cm. In contrast, significant negative responses were observed in deep soils (30-100 cm) for *Populus* spp planted forests. The afforestation group of other tree species did not show significant SIC changes for all the depths.

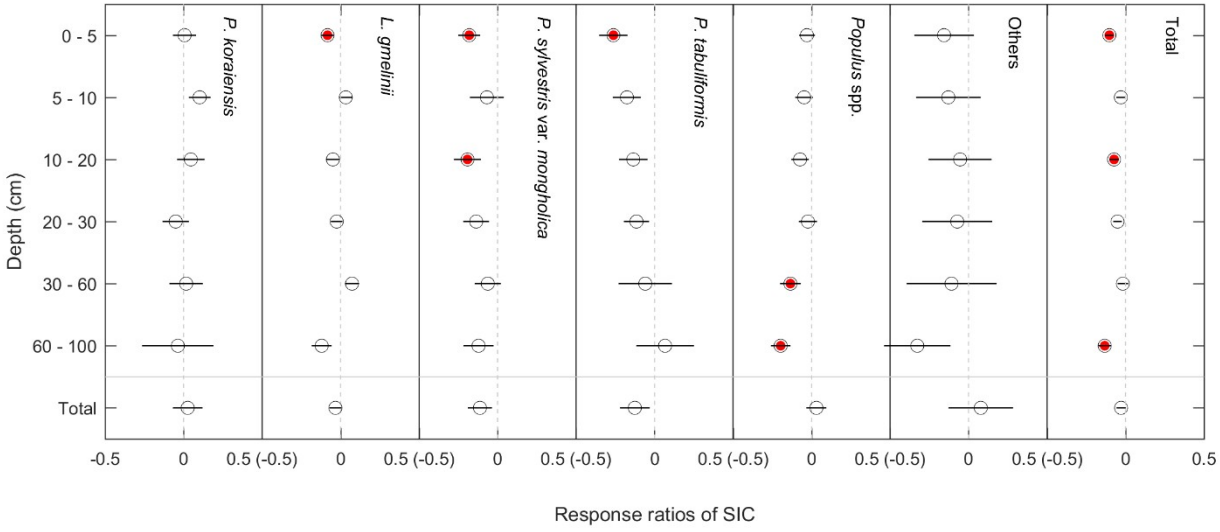

Figure 3. The response ratio (RR) of soil inorganic carbon (SIC) to afforestation with different tree species at different depth. Error bars indicate the standard errors. Red points indicate the RRs are significantly different from 0 ($p < 0.05$) in independent sample *t*-tests, with FDR corrections.

3.2 Factors controlling the dynamics of SIC after afforestation

Using SEM to quantify the direct and indirect effects of different environmental factor on afforestation-caused SIC dynamics, we found that ΔpH (Change of soil pH resulted from afforestation) was the most significant variable (β = 0.42, standardized coefficient, $p < 0.001$) determining RR_SIC. Changes of SOC (ΔSOC) also showed a significant effect (β = 0.12, $p < 0.01$) on the RR_SIC. Hence, afforestation impacts the dynamics of SIC mainly through changing soil pH and SOC. The background soil pH (pH_c) and SIC also had significant impacts on SIC changes, with pH_c showing a positive effect (β = 0.19, $p < 0.01$) while SIC_c a negative one (β = -0.31, $p < 0.001$). Direct effects of other variables, including MAT, water balance, nitrogen deposition,

303 background SOC, clay content, and stand age, on RR_SIC were weak and
304 nonsignificant. However, these variables could affect SIC dynamics indirectly through
305 affecting the dynamics of soil pH and SOC.

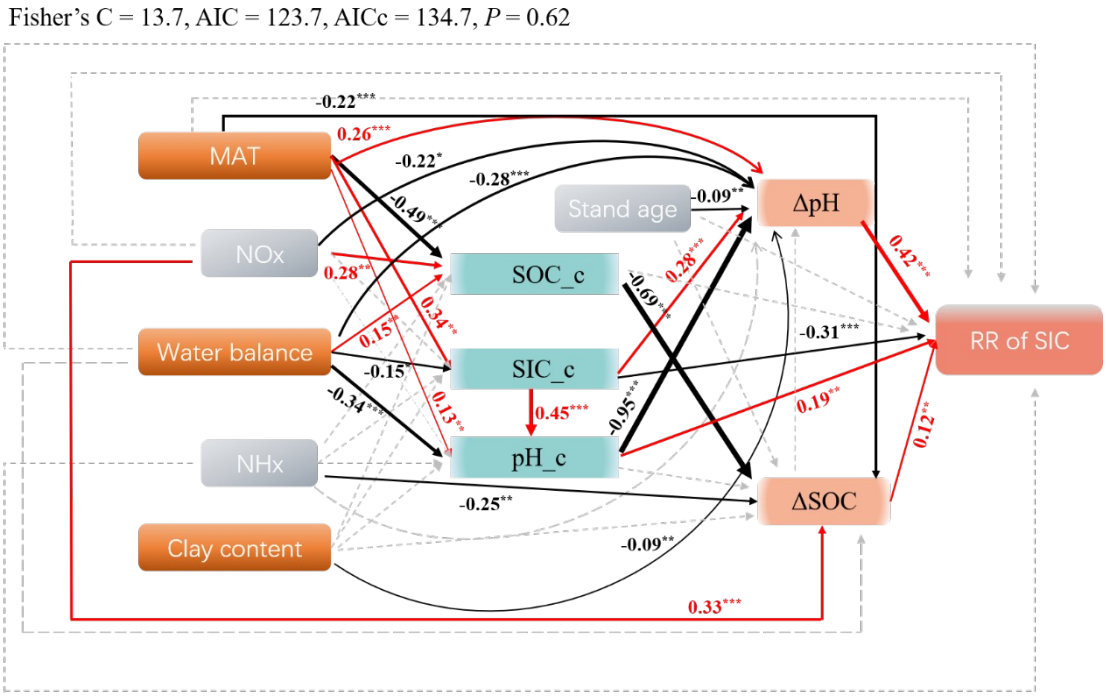

306

307 **Figure 4.** Structure equation model for the response ratio (RR) of soil inorganic
308 carbon (SIC). Solid red and black arrows represent significantly ($p < 0.05$) positive
309 and negative paths, respectively; and gray dashed lines indicate nonsignificant
310 pathways. The numbers near the lines indicate the standard path coefficients. Arrow
311 widths is proportional to the strength of the relationship.

312

313 Next, we also analyzed the correlations between RR_SIC and its most important
314 determining factor revealed by the SEM, ΔpH. Individually, ΔpH showed a strong
315 positive effect on RR_SIC (Figure 5a, $p< 0.001$), which was also mediated by pH in
316 the control group (pH_c). Negative RR_SIC values were usually observed at alkaline

317 (high pH) soils, where afforestation generally decreased soil pH. In contrast, positive
318 values of RR_SIC were generally observed at acidic (low pH) soils, where soil pH
319 usually increased after afforestation. The absolute change of SIC (ΔSIC) was also
320 positively correlated with ΔpH (Figure 5b), and the sensitivity (regression slope
321 between ΔSIC and ΔpH) increased with background soil pH. In other words, SIC in
322 more alkaline soils was more sensitive to the change of soil pH than that in acidic
323 soils.

324 Interestingly, larger changes in SIC density was mainly found in arid areas where
325 SIC stocks were usually high as well (Figure S1). In areas with SIC density higher
326 than 1 kgC m^{-2}, ΔSIC was negatively correlated with water balance (MAP – PET).
327 The largest loss of SIC was observed in areas with water deficiency of about 200 mm
328 yr^{-1}.

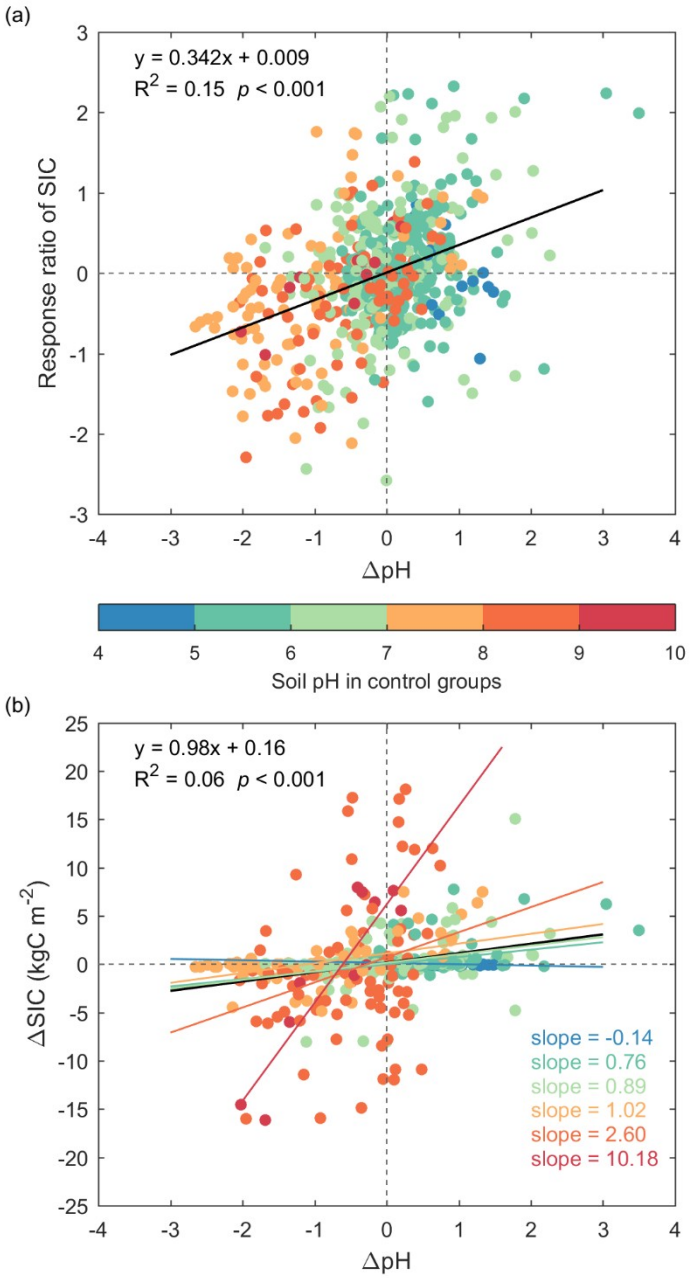

329

330 **Figure 5.** The relationships between ΔpH (pH in afforested groups – pH in control
331 groups) and (a) response ratio (RR) of soil inorganic carbon (SIC) and (b) ΔSIC (SIC
332 in afforested groups – SIC in control groups). Two panels share the same color bar,
333 which indicates soil pH in control groups. The red lines indicate the results of
334 ordinary least squares (OLS) regressions.

335

336 The determinant of soil pH on the dynamics of SIC was observed for all tree
337 species (Figure 6). Negative RR_SIC was generally observed when soil pH was
338 higher than 7, where *Larix gmelinii* showed the most significant negative response.
339 When soil pH was lower than 7, positive RR_SIC was commonly observed, and the
340 "others" afforestation group showed the most significant positive response (Figure
341 6a). Taking ΔSIC into consideration, afforestation with *Larix gmelinii*, *Pinus*
342 *tabuliformis* and the "others" group resulted in the largest carbon loss at soils with
343 pH> 8; while *Pinus koraiensis* and the group of "others" had the largest carbon sink at
344 soils with pH< 7 (Figure 6b). Soil pH, tree species and their interactions all had
345 significant effects on the changes of SIC (two-way ANOVA, $p < 0.05$).

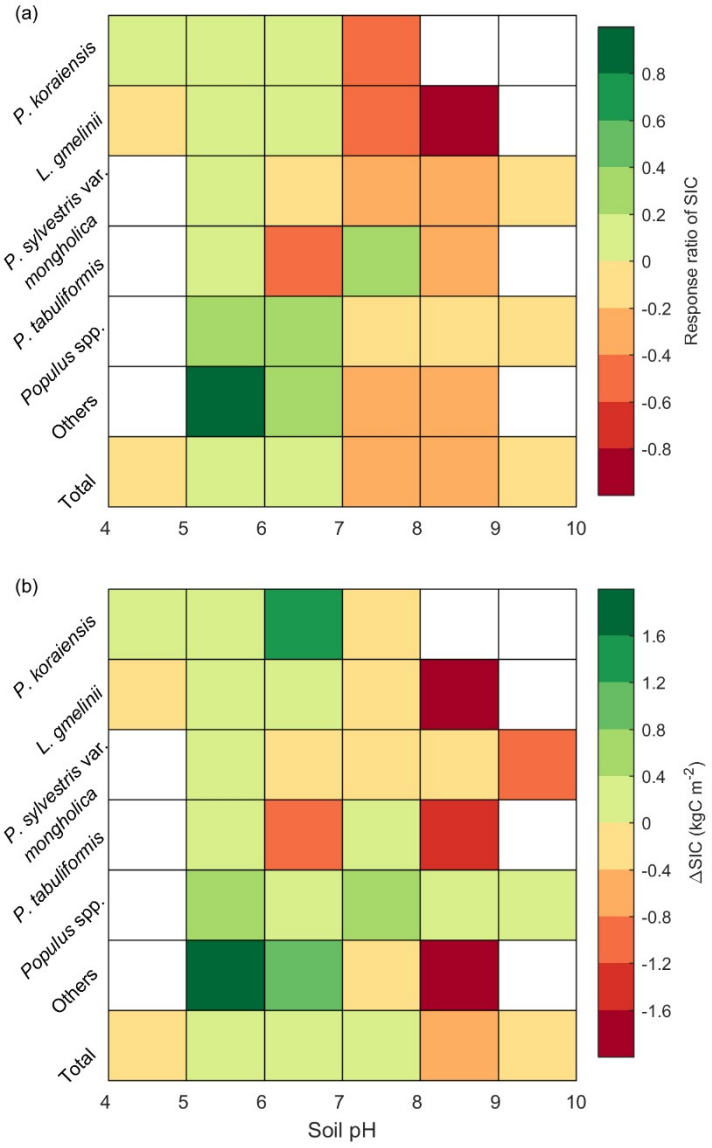

346

347 **Figure 6.** (a) Response ratio (RR) of soil inorganic carbon (SIC) and (b) ΔSIC among

348 different tree species and different soil pH in control groups.

349

350 **3.3 Contribution of SIC to soil carbon dynamics after afforestation**

351 Across the whole region, the averaged change of SIC was 0.05 kgC m^{-2} (SD =

352 3.23) and insignificant from 0 (p = 0.71), smaller than the mean value of ΔSOC (0.30

353 kgC m^{-2}). Both positive and negative responses of SOC and SIC were observed, but

we did not find any significant relationships between them (Figure S2). Given the divergent responses of SIC and SOC, we divided the soil carbon dynamics into four scenarios: positive ΔSOC and positive ΔSIC, positive ΔSOC and negative ΔSIC, negative ΔSOC and positive ΔSIC, negative ΔSOC and negative ΔSIC. Positive ΔSOC and positive ΔSIC were observed in 159 out of 619 pairs. In this group, mean values of ΔSOC and ΔSIC were 6.57 and 1.46 kgC m^{-2}, respectively. Negative ΔSOC and positive ΔSIC were observed at 131 pairs, where their mean values were -5.02 and 1.56 kgC m^{-2}, respectively. Similarly, positive ΔSOC and negative ΔSIC were observed at 162 pairs, with mean values of 5.17 and -1.51 kgC m^{-2}, respectively. And both negative ΔSOC and ΔSIC were observed in the remaining 167 pairs, with averaged values of -6.22 and -0.97 kgC m^{-2}, respectively.

The change of SIC contributed differentially to soil carbon dynamics across different tree species (Figure 7). In *Pinus koraiensis* and *Larix gmelinii* afforestations, SIC contributed very little to soil carbon dynamics. In forests of *Pinus sylvestris* var. *mongholica*, changes in SIC made a substantial contribution to the total soil carbon dynamics at sites with positive ΔSOC. Finally, the changes of SIC and SOC showed similar contributions to the total soil carbon dynamics for the afforestation groups of *Pinus tabuliformis*, and *Populus* spp. and others.

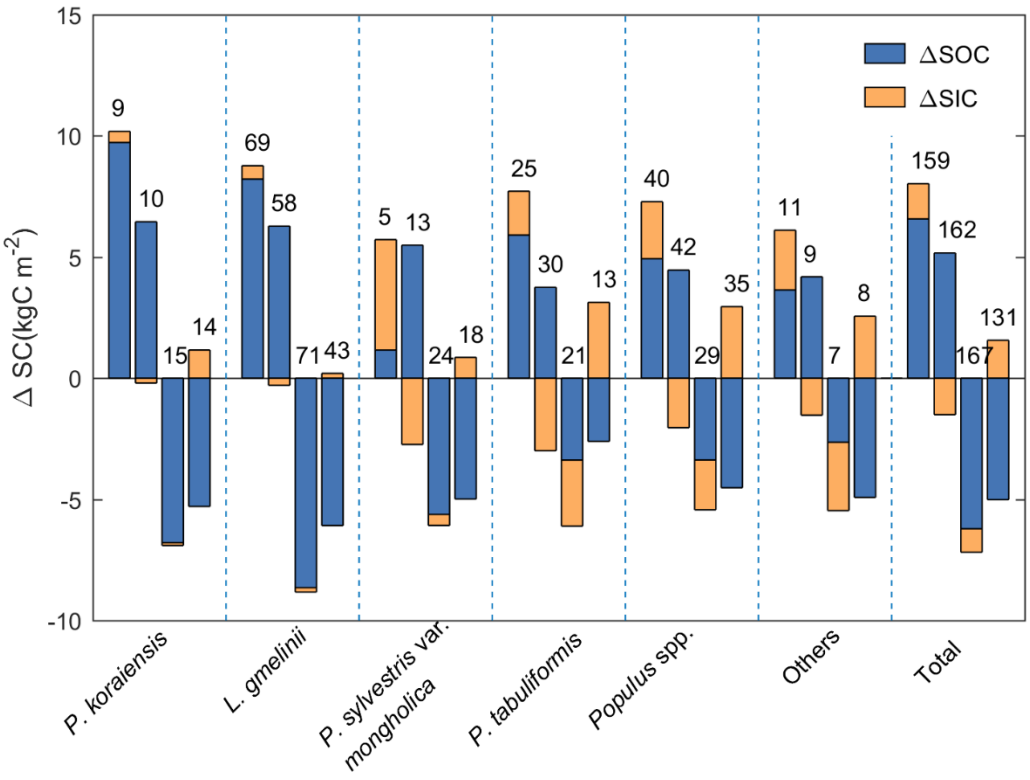

Figure 7. ΔSIC and ΔSOC resulted from afforestation with different tree species. For each tree species, four groups (positive ΔSIC and ΔSOC, positive ΔSIC and negative ΔSOC, negative ΔSIC and positive ΔSOC, negative ΔSIC and ΔSOC) are contained. The numbers near the bar indicate the sample size of each group.

4. Discussion

With field data collected from more than 700 plots over a broad geographical range in northern China, we provided a comprehensive evaluation on the effects of afforestation on SIC, an often-overlooked quantity in the research of carbon cycle dynamics. In general, we found that afforestation had divergent effects on SIC, dependent on afforestation tree species and soil depths. However, for those species and soil depths that showed a significant impact, it was always negative (Figure 3).

This negative impact was mostly observed at surface soil layers. Therefore, our finding suggested that SIC, especially surface SIC, is still sensitive to possible soil biophysical and biogeochemical environmental changes caused by afforestation.

In explaining the relative change of SIC with afforestation, we found that RR_SIC is well correlated with ΔpH, indicating the sensitivity of SIC to changes in soil pH (Liu et al., 2020). Given that pH value is the negative logarithm of hydrogen ion, this correlation between RR_SIC and ΔpH indicates that the dynamics of SIC and hydrogen ion are synergetic, also consistent with our earlier finding from a spatial analysis (Hong et al., 2019). Soil pH and SIC are closely linked at local and regional scales, and SIC provides major buffering capacity to soil pH especially at arid area (Hong et al., 2019). At the local scale, changes in soil pH could also impact the decomposition and formation of SIC. Interestingly, our analysis based on SEM suggested contrast direct versus indirect effects of the background soil pH (pH_c) on RR_SIC. The positive direct effect of pH_c indicates that higher pH would directly enhance post-afforestation SIC. However, because afforestation has been found to increase soil pH at acid soil but decrease soil pH at alkaline soil (Hong et al., 2018), for SIC stored in alkaline soils in the form of carbonate, this afforestation-induced soil acidification could partly dissolve SIC (Raza et al., 2020), leading to a negative indirect effect. Importantly, this indirect negative effect is much stronger than the direct positive effect of pH_c, resulting in significant SIC losses by afforestation in area with high pH values. This mechanism also explains the finding of the large carbon loss in SIC-rich soils during 1980s to 2000s by an early study (Yang et al.,

2012b).

Afforestation-induced changes in SOC provides another pathway modifying the response of SIC. The accumulation of SOC will increase CO_2, base cations like Ca^{2+}, Mg^{2+}, which restrain the dissolution of SIC and enhance the formation of SIC (An et al., 2019). The organic acid produced by the decomposition of SOC may also affect soil pH and thus SIC (Hong et al., 2018), although in the current study this effect was weak and nonsignificant.

Other environmental variables, such as nitrogen deposition and water balance, seem to have weak or insignificant effects on RR_SIC. For example, although nitrogen deposition has been found to help regulate the spatial patterns of SIC and pH (Hong et al., 2019), the difference of nitrogen deposition between adjacent control and afforested plots may not be captured by the data with a resolution of 0.5°x0.5° (Wei et al., 2014). The hydrological effects of afforestation could also affect the carbonate leaching in soil profiles and lead to SIC vertical redistribution (Li et al., 2019). However, SIC loss is generally observed in arid areas, where the leaching effect is very weak (Chang et al., 2012). Previous studies also indicated that the vertical reallocation was limited (Li et al., 2019).

Although a few previous studies have investigated SIC dynamics, they were generally confined to arid areas with high soil pH and large SIC stocks (Yang et al., 2012a; An et al., 2019). Our study, in contrast, provided for the first time a field data-based analysis of SIC changes with afforestation across a broad range of climates from arid to humid areas. Our results indicated that the relative change of SIC was

close related to soil pH dynamics across the water deficit gradient, with the absolute change of SIC more sensitive to afforestation-induced pH change in soils with higher pH and SIC stocks. This higher sensitivity of alkaline SIC to afforestation may be due to the greater availability of substrates for soil pH neutralization reactions. Considering the significant acidification resulted from afforestation in alkaline soils (Hong et al., 2018), these results indicate the high vulnerability of SIC in arid areas. Therefore, areas with high SIC stocks should be carefully evaluated for afforestation to minimize potential soil carbon loss.

The loss of SIC to afforestation could be harmful to soil health and ecosystem productivity (Skyllberg, 1996; Bowman et al., 2008). In arid ecosystems, SIC plays an even more important role in carbon storage (Han et al., 2018). SIC, in the form of carbonate, also provides the major buffering capacity to soil pH change in these regions (Bowman et al., 2008). The decrease of SIC by afforestation may indicate the reduction of soil buffering capacity. Considering the high risk of soil acidification caused by increasing nitrogen and sulfur deposition in these regions, this reduction of soil buffering capacity may lead to a positive feedback between soil acidification and carbonate loss (Yang et al., 2012a; Ito et al., 2018). Carbonate dissolution drives the losses of base cations such as Ca^{2+}, Mg^{2+} and K^{+}, and further decreases soil fertility (Liu et al., 2020). A global meta-analysis suggested that afforestation resulted in a significant loss of base cations, especially in pine plantations (Berthrong et al., 2009). Given the essential role of exchangeable base cations for plant physiological processes, their loss would limit the long-term productivity of ecosystems (Binkley et

al., 1989). Moreover, SIC loss would decrease the binding of organic matters on Ca^{2+}, and thus decrease its stability (Rowley et al., 2017). Therefore, the dynamic of SIC plays an important role in global carbon cycle and ecosystem health through direct and indirect ways, and afforestation-caused SIC losses should be avoided as much as possible.

Large-scale afforestation is regarded as an effective ecological engineering approach for increasing ecosystem carbon storage and mitigating climate change. The augmentation of planted forests worldwide is known to regulate local climate, reduce soil erosion, increase carbon storage in plant biomass and potentially also SOC (Li et al., 2017; Li et al., 2018). Our findings, however, suggest that afforestation significantly impacts SIC storage, primarily through affecting soil pH. This finding again questions the earlier belief that SIC stocks are very stable and play a minor role in global carbon cycle. For some afforestation tree species, such as *Pinus sylvestris* var. *mongholica, Pinus tabuliformis and Populus* spp., the changes of SIC are even comparable to SOC, suggesting that the estimation of carbon dynamics in this rapidly changing world should not neglect that of SIC. The total carbon sequestration of afforestation (including biomass, SOC and SIC) are thus highly variable, determined by climate, soil properties, tree species choices and also human-based management. Therefore, the estimation that afforestation has the potential to offset 68% of global CO_2 emissions is highly uncertain and may be overly optimistic (Bastin et al., 2019). Furthermore, the climate and soil conditions need to be carefully evaluated and the planted tree species need to wisely chosen for maximizing the benefits while

474 minimizing potential detriments of afforestation.

475

476

477 **Acknowledgements**

478 This study was partly supported by the National Key R&D Program of China
479 (2017YFA0604702) and the Strategic Priority Research Program (A) of the Chinese
480 Academy of Sciences (grant XDA20050101). A.C. also acknowledges the support
481 from Colorado State University.

482

483 **Data Availability Statement**: All field data related to this research will be archived in
484 the Dryad repository upon the acceptance of this manuscript for publication.

485

486 **Reference**

487 Ahirwal, J. & Maiti, S.K. (2018). Assessment of soil carbon pool, carbon
488 sequestration and soil CO2 flux in unreclaimed and reclaimed coal mine
489 spoils. *Environmental Earth Sciences*, **77**: 9.

490 An, H., Wu, X., Zhang, Y. & Tang, Z. (2019). Effects of land-use change on soil
491 inorganic carbon: A meta-analysis. *Geoderma*, **353**, 273-282.

492 Barak, P., Jobe, B.O., Krueger, A.R., Peterson, L.A. & Laird, D.A. (1997). Effects of
493 long-term soil acidification due to nitrogen fertilizer inputs in Wisconsin.
494 *Plant and Soil*, **197**, 61-69.

495 Bastin J. F. Finegold, Y., Garcia, C., Mollicone, D., Rezende, M., Routh, D. et al.
496 (2019). The global tree restoration potential. *Science*, **365**, 76-79.

497 Benjamini, Y. & Yekutieli, D. (2001). The control of false discovery rate in multiple
498 testing under dependency. *Annals of Statistics*, **4**, 1165–1188.
499 Berthrong, S.T., Jobbágy, E.G. & Jackson, R.B. (2009). A global meta-analysis of soil
500 exchangeable cations, pH, carbon, and nitrogen with afforestation. *Ecological*
501 *Applications*, **19**, 2228-2241.
502 Binkley, D., Valentine, D., Wells, C. & Valentine, U. (1989). An empirical analysis of
503 the factors contributing to 20-year decrease in soil pH in an old-field
504 plantation of loblolly pine. *Biogeochemistry*, **8**, 39-54.
505 Bonan, G.B. (2008). Forests and Climate Change: Forcings, Feedbacks, and the
506 Climate Benefits of Forests. *Science*, **320**, 1444-1449.
507 Bowman, W.D., Cleveland, C.C., Halada, L., Hresko, J. & Baron, J.S. (2008).
508 Negative impact of nitrogen deposition on soil buffering capacity. *Nature*
509 *Geoscience*, **1**, 767-770.
510 Bughio, M.A., Wang, P., Meng, F., Chen, Q., Li, J. & Shaikh, T.A. (2017).
511 Neoformation of pedogenic carbonate and conservation of lithogenic
512 carbonate by farming practices and their contribution to carbon sequestration
513 in soil. *Journal of Plant Nutrition and Soil Science*, **180**, 454-463.
514 Bughio, M.A., Wang, P., Meng, F., Qing, C., Kuzyakov, Y., Wang, X. et al. (2016).
515 Neoformation of pedogenic carbonates by irrigation and fertilization and their
516 contribution to carbon sequestration in soil. *Geoderma*, **262**, 12-19.
517 Chang, R., Fu, B., Liu, G. & Liu, S. (2011). Soil Carbon Sequestration Potential for
518 "Grain for Green" Project in Loess Plateau, China. *Environmental*

519 *Management*, **48**, 1158-1172.
520 Chang, R., Fu, B., Liu, G., Wang, S. & Yao, X. (2012). The effects of afforestation on
521 soil organic and inorganic carbon: A case study of the Loess Plateau of China.
522 *Catena*, **95**, 145-152.
523 Chen, Y., Yang, K., He, J., Qin, J., Shi, J., Du, J. et al. (2011). Improving land surface
524 temperature modeling for dry land of China. *Journal of Geophysical*
525 *Research-Atmospheres,* **116**, D20104.
526 Cheng, J., Lee, X., Tang, Y., Pan, W., Gao, W., Chen, Y. et al. (2016). Changes in
527 above- and below-ground nitrogen stocks and allocations following the
528 conversion of farmland to forest in rocky desertification regions. *Agriculture*
529 *Ecosystems & Environment*, **232**, 9-16.
530 Fang, H. & Sun, L. (2017). Modelling soil erosion and its response to the soil
531 conservation measures in the black soil catchment, Northeastern China. *Soil &*
532 *Tillage Research*, **165**, 23-33.
533 Fang, J. & Chen, A. (2001). Dynamic forest biomass carbon pools in China and their
534 significance. *Acta Botanica Sinica*, **43**(9): 967-973.
535 Fang, J., Chen, A., Peng, C., Zhao, S. & Ci, L. (2001). Changes in Forest Biomass
536 Carbon Storage in China Between 1949 and 1998. *Science*, **292**, 2320-2322.
537 FAO. Global Forest Resources Assessment 2015. Rome, Italy: Food and Agricultural
538 Organization of the United Nations (2016).
539 Gundersen, P., Schmidt, I. & Raulund-Rasmussen, K. (2011). Leaching of nitrate from
540 temperate forests - effects of air pollution and forest management.

Environmental Reviews **14**(1):1-57.

Guo, J.H., Liu, X.J., Zhang, Y., Shen, J.L., Han, W.X., Zhang, W.F., et al. (2010). Significant Acidification in Major Chinese Croplands. *Science*, **327**, 1008-1010.

Han, X., Gao, G., Chang, R., Li, Z., Ma, Y., Wang, S. et al. (2018). Changes in soil organic and inorganic carbon stocks in deep profiles following cropland abandonment along a precipitation gradient across the Loess Plateau of China. *Agriculture Ecosystems & Environment*, **258**, 1-13.

Harris, I., Jones, P., Osborn, T. & Lister, D. (2014). Updated high-resolution grids of monthly climatic observations—The CRU TS3.10 Dataset.

HÖGberg, P., Fan, H., Quist, M., Binkley, D.A.N. & Tamm, C.O. (2006). Tree growth and soil acidification in response to 30 years of experimental nitrogen loading on boreal forest. *Global Change Biology*, **12**, 489-499.

Hong, S., Gan, P. & Chen, A. (2019). Environmental controls on soil pH in planted forest and its response to nitrogen deposition. *Environmental Research*, **172**, 159-165.

Hong, S., Piao, S., Chen, A., Liu, Y., Liu, L., Peng, S. et al. (2018). Afforestation neutralizes soil pH. *Nature Communications*, **9**, 520.

Hong, S., Yin, G., Piao, S., Dybzinski, R., Cong,. N., Li, X., et al. (2020). Divergent responses of soil organic carbon to afforestation. *Nature Sustainability* **3**, 694–700.

IPCC (Intergovernmental Panel on Climate Change). Fifth Assessment Report. IPCC.

563 http://ipcc.ch/report/ar5/ (2014).
564 Ito, A., Nishina, K., Ishijima, K., Hashimoto, S. & Inatomi, M. (2018). Emissions of
565 nitrous oxide (N2O) from soil surfaces and their historical changes in East
566 Asia: a model-based assessment. *Progress in Earth and Planetary Science*,
567 **5**:55.
568 Jia, X., Wang, X., Hou, L., Wei, X., Zhang, Y., Shao, M. et al. (2019). Variable
569 response of inorganic carbon and consistent increase of organic carbon as a
570 consequence of afforestation in areas with semiarid soils. *Land Degradation &*
571 *Development*, **30**, 1345-1356.
572 Kim, J., Jobbágy, E., Richter, D., Trumbore, S. & Jackson R. (2020) Agricultural
573 acceleration of soil carbonate weathering. *Global Change Biology*, **26**: 5988–
574 6002.
575 Lal, R. (2004). Soil Carbon Sequestration Impacts on Global Climate Change and
576 Food Security. *Science*, **304**, 1623-1627.
577 Li, D., Wen, L., Zhang, W., Yang, L., Xiao, K., Chen, H. et al. (2017). Afforestation
578 effects on soil organic carbon and nitrogen pools modulated by lithology.
579 *Forest Ecology and Management*, **400**, 85-92.
580 Li, H., Shen, H., Zhou, L., Zhu, Y., Chen, L., Hu, H. et al. (2019). Shrub
581 encroachment increases soil carbon and nitrogen stocks in temperate
582 grasslands in China. *Land Degradation & Development*, **30**, 756-767.
583 Li, Y., Piao, S., Li, L.Z.X., Chen, A., Wang, X., Ciais, P., et al. (2018). Divergent
584 hydrological response to large-scale afforestation and vegetation greening in

China. *Science Advances*, **4,** :eaar4182.

Li, Y., Piao, S., Chen, A., Ciais, P. & Li, L.Z.X. (2020). Local and teleconnected temperature effects of afforestation and vegetation greening in China. *National Science Review,* **7**: 897–912.

Lian, X., Piao, S., Chen, A., Huntingford, C., Fu, B., Li, L.Z.X. et al., (2021). Multifaceted characteristics of dryland aridity changes in a warming world. *Nature Reviews Earth & Environment,* **2**, 232–250.

Liu, S., Zhou, L., Li, H., Zhao, X., Yang, Y., Zhu, Y. et al. (2020). Shrub encroachment decreases soil inorganic carbon stocks in Mongolian grasslands. *Journal of Ecology*, **108**, 678-686.

Pan, Y., Birdsey, R., Fang, J., Houghton, R., Kauppi, P., Kurz, W. et al. (2011). A Large and Persistent Carbon Sink in the World's Forests. *Science*. **333**, 988-993.

Peng, S., Piao, S., Zeng, Z., Ciais, P., Zhou, L., Li, L.Z.X. et al. (2014). Afforestation in China cools local land surface temperature. *Proceedings of the National Academy of Sciences*, **111**, 2915-2919.

Piao, S., Fang, J., Zhu, B. & Tan, K. (2005). Forest biomass carbon stocks in China over the past 2 decades: Estimation based on integrated inventory and satellite data. *Journal of Geophysical Research-Biogeosciences*, **110,** G01006.

Piao, S., Fang, J., Ciais, P., Peylin, P., Huang, Y., Sitch, S. et al. (2009). The carbon balance of terrestrial ecosystems in China. *Nature*, **458**, 1009-1013.

Piao, S., Huang, M., Liu, Z., Wang, X., Ciais, P., Canadell, J. et al. (2018). Lower land-use emissions responsible for increased net land carbon sink during the

607 slow warming period. *Nature Geoscience,* **11**, 739–743.
608 Raza, S., Na, M., Wang, P., Ju, X., Chen, Z., Zhou, J. et al. (2020). Dramatic loss of
609 inorganic carbon by nitrogen-induced soil acidification in Chinese croplands.
610 *Global Change Biology*, **26**, 3738-3751.
611 Rhoades, C. & Binkley, D. (1996). Factors influencing decline in soil pH in Hawaiian
612 Eucalyptus and Albizia plantations. *Forest Ecology and Management.* **80**, 47–
613 56.
614 Rowley, M.C., Grand, S. & Verrecchia, E. (2017). Calcium-mediated stabilisation of
615 soil organic carbon. *Biogeochemistry*, **137**, 27-49.
616 Schlesinger, W.H. (1990). Evidence from chronosequence studies for a low carbon-
617 storage potential of soils. *Nature*, **348**, 232.
618 Schlesinger, W.H. & Andrews, J.A. (2000). Soil respiration and the global carbon
619 cycle. *Biogeochemistry*, **48**, 7-20.
620 Skyllberg, U. (1996). Small scale pH buffering in organic horizons of two boreal
621 coniferous forest stands. *Plant and Soil*, **179**, 99-107.
622 Slessarev, E., Lin, Y., Bingham, N., Johnson, J., Dai, Y., Schimel, J. et al., (2016).
623 Water balance creates a threshold in soil pH at the global scale. *Nature* **540**,
624 567–569.
625 Tian, D. & Niu, S. (2015). A global analysis of soil acidification caused by nitrogen
626 addition. *Environmental Research Letters*, **10**, 024019.
627 Wei, Y., Liu, S., Huntzinger, D., Michalak, A., Viovy, N., Post, W. et al., (2014).
628 NACP MsTMIP: global and North American driver data for multimodel
629 intercomparison (ORNL DAAC); https://doi.org/10.3334/ORNLDAAC/1220.

630 Xie, Z., Zhu, J., Liu, G., Cadisch, G., Hasegawa, T., Chen, C. et al., 2007. Soil organic
631 carbon stocks in China and changes from 1980s to 2000s. *Global Change*
632 *Biology,* **13**, 1989–2007.
633 Xiong, Y. & Li, Q., 1987. Soils in China. Press of Sciences, Beijing.
634 Yang, K., He, J., Tang, W., Qin, J. & Cheng, C.C.K. (2010). On downward shortwave
635 and longwave radiations over high altitude regions: Observation and modeling
636 in the Tibetan Plateau. *Agricultural and Forest Meteorology*, **150**, 38-46.
637 Yang, Y., Ji, C., Ma, W., Wang, S., Wang, S., Han, W. et al. (2012a). Significant soil
638 acidification across northern China's grasslands during 1980s–2000s. *Global*
639 *Change Biology*, **18**, 2292-2300.
640 Yang, Y., Fang, J., Ji, C., Ma, W., Mohammat, A., Wang, S. et al. (2012b). Widespread
641 decreases in topsoil inorganic carbon stocks across China's grasslands during
642 1980s-2000s. *Global Change Biology*, **18**, 3672-3680.
643 Yao, Y., Zeng, Z., Liu, Y., Peng, S., Zhu, Z. & Piao S. (2016). The Effect of
644 Afforestation on Soil Moisture Content in Northeastern China. *PLoS ONE,* **11**,
645 e016776.
646 Zamanian, K., Zarebanadkouki, M. & Kuzyakov, Y. (2018) Nitrogen fertilization
647 raises CO2 efflux from inorganic carbon: A global assessment. *Global Change*
648 *Biology*, **24**, 2810-2817.
649 Zhao, Y., Duan, L., Xing, J., Larssen, T., Nielsen, C. & Hao I. (2009). Soil
650 acidification in China: is controlling SO2 emissions enough? *Environ. Sci.*
651 *Technol.* **43**, 8021–8026.